Full-Color OLEDs Integrated by Dry Dye Printing

K. Long, *Member, IEEE*, F. Pschenitzka, M.-H. Lu, *Member, IEEE*, and James C. Sturm, *Fellow, IEEE*

***Abstract*—Dry dye printing and solvent-enhanced dye diffusion were used to locally dope a previously spin-coated poly(9-vinylcarbazole) (PVK) polymer film with different dyes to fabricate side-by-side red, green, and blue (RGB) organic light-emitting device pixels. The fabrication details and the resolution and stability of this patterning technique are discussed. The technique was then used to make combined polymer/small-molecule devices, in which the printability of polymer for color integration was combined with the superior transport properties and thin-layer capabilities of small molecules for high efficiency and low leakage current. To reduce reverse leakage current and raise efficiency, a blanket tris-8-hydroxyquinoline aluminum (Alq_3) electron transport layer was deposited on top of the polymer layer after the dye diffusion step, along with a 2,9-dimethyl-4,7-diphenyl-1,10-phenanthroline hole/exciton blocking layer between the Alq_3 and the PVK to ensure that all light emission occurred from the doped polymer and not from the Alq_3. Devices with this hybrid doped polymer/small molecule structure have an extremely low reverse leakage current (with a rectification ratio of 10^6 at ± 10 V). The electroluminescence efficiency of the devices was optimized by varying the dye concentration of the printing plate. A three-color passive-matrix test array with 300 μm $\times$ 1 mm RGB subpixels was demonstrated with this structure.**

***Index Terms*—Flat-panel displays, full color, organic light-emitting diode (OLED) integration, OLED, passive matrix, printing.**

I. Introduction

THE FIRST commercial display products based on polymer organic light-emitting diodes (OLEDs) are in the process of being introduced to the market. Polymers are attractive emission materials for OLED displays because they can be deposited by low-cost and high-throughput methods such as spin coating. However, spin coating creates blanket layers that can generally emit only one color. For efficient full-color displays, pixels emitting red, green, and blue (RGB) colors should be fabricated side by side on the same substrate with high resolution. Therefore, patterning the polymer layer to achieve RGB colors is critical.

The emission colors of polymers can be controlled by adding a small amount of fluorescent dyes into the polymer films (less than 1% by weight) [1], [2]. There are several methods to achieve full color based on this principle, for example, ink-jet printing of a dye solution on a previously spin-coated polymer film [3], photobleaching of a dye [4], patterned dye transfer by local heating [5], and thermal transfer through a mask [6]. More recently, we have focused on a local dry dye transfer process with two steps, where the dye is first printed onto the device polymer surface using a patterned soft printing plate, followed by diffusion into the polymer film [7]. To lower the temperature required to uniformly diffuse the dye throughout the device polymer from over 100 °C to room temperature, a solvent-vapor annealing step has been adopted [8], [9].

Dry printing is in principle attractive compared to wet printing such as ink-jet since issues associated with the lateral redistribution during the solvent drying process can be avoided [10], [11]. A large-area highly parallel printing process is also attractive from a throughput point of view compared to a serial process such as ink-jet printing [12], [13]. This paper extends the local dye transfer process to pattern polymer over large area and demonstrates operation of a three-color pixel. Both technology problems associated with the dye patterning process (Section II) as well as device efficiency and optimization (Section III) are addressed.

II. Large-Area Dye Printing Into Polymers

A. Process Overview

The solvent-enhanced dry-dye-printing method is shown schematically in onto which the polymer is uniformly deposited by spin coating from a chlorobenzene solution to form a 90-nm-thick film. In all of the work in this paper, the solution contained poly(9-vinylcarbazole) (PVK, M_w ca. 1 100 000 g/mol; 71% by weight in the final film) as the host polymer and the hole transport material, 2-(4-biphenylyl)-5-(4-*tert*-butyl-phenyl)-1, 3, 4,-oxidiazole (PBD; 28.7% by weight) as the electron transport molecule and the blue dye Coumarin 47 (C47; 0.3% by weight, emission peak at 440 nm) as the blue emission material [2], unless noted otherwise.

The printing plate consists of a prepatterned dye source layer on a glass substrate. The dye source layer consists of a polymer matrix of Vylon 103 to which the green dye Coumarin 6 (C6, emission peak at 500 nm) or red dye Nile red (NR, emission peak at 590 nm) was added. The fabrication of this printing plate is discussed below. The printing plate was aligned to and brought into contact with the device plate and then annealed in vacuum at 70 °C for 1 h to transfer the dyes from the dye source

Manuscript received November 30, 2005; revised April 4, 2006. This work was supported by the Defense Advanced Research Projects Agency under Grant MDA972-00-3-0002 (with Planar Systems F33615-98-1-5164) and the New Jersey Commission on Science and Technology under Grant NJOOE03-2041-007-11. The review of this paper was arranged by Editor J. Kanicki.

K. Long and J. C. Sturm are with the Department of Electrical Engineering, Princeton Institute for the Science and Technology of Materials, Princeton University, Princeton, NJ 08544 USA (e-mail: kelong@princeton.edu).

F. Pschenitzka is with the Department of Electrical Engineering, Princeton Institute for the Science and Technology of Materials, Princeton University, Princeton, NJ 08544 USA. He is also with the Cambrios Technologies Corporation, Mountain View, CA 94043 USA.

M.-H. Lu is with the Department of Electrical Engineering, Princeton Institute for the Science and Technology of Materials, Princeton University, Princeton, NJ 08544 USA. He is also with the Universal Display Corporation, Princeton Crossroads Corporate Center, Ewing, NJ 08618 USA.

Digital Object Identifier 10.1109/TED.2006.879021

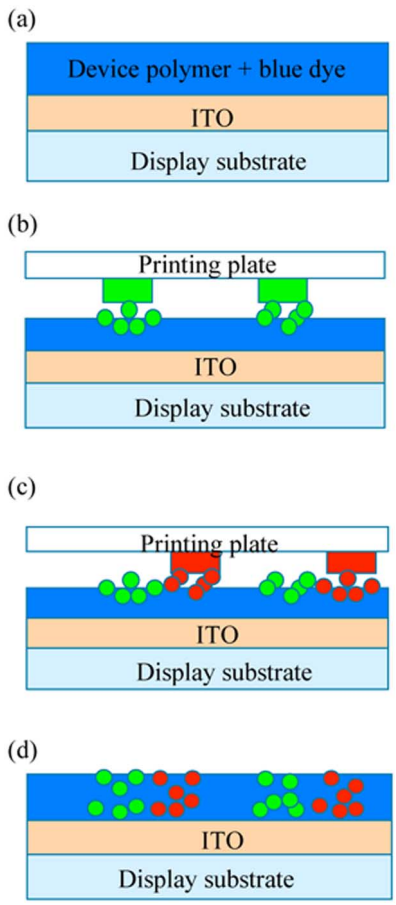

Fig. 1. Schematic process flow of dry dye printing from prepatterned dye sources and subsequent solvent-enhanced dye diffusion for RGB patterns. (a) Uniform spin coat of device polymer with blue dye. (b) Transfer of green dye from prepatterned dye source (at 70 °C for 1 h). (c) Repeat the transfer step for red dye. (d) Solvent-enhanced diffusion of dye throughout the polymer film. Vertical dimensions are exaggerated versus lateral dimensions.

onto the surface of the device polymer. This initial dye transfer step was done once for the green dye and once for the red dye. Then, the device sample was put into an acetone vapor ambient to diffuse the dyes throughout the bulk of the polymer film. A uniform dye distribution throughout the polymer film was achieved after a treatment in acetone vapor for 150 s at room temperature in a nitrogen atmosphere with 130 ml gaseous acetone per liter of gaseous N_2 [7]. The device structure and subsequent processing are discussed in a later section of this paper (see Section III).

B. Printing Plate Fabrication

The printing plates (Fig. 1) consist of a glass substrate and a dye-doped polymer layer as the dye source. The uniform dye source layer is formed by spin coating from a solution containing polymer Vylon 103 (obtained from Toyoba, M_w 20 000–25 000 g/mol; glass transition temperature $T_g = 47$ °C) and the green dye C6 or the red dye NR to be diffused into the device polymer layer. The dye concentration was varied from 2% to 8% by weight in Vylon. Vylon is used because of its low glass transition temperature, which allows dye to diffuse out easily, and its "antistick" properties, which causes it not to stick to the device polymer during the printing process.

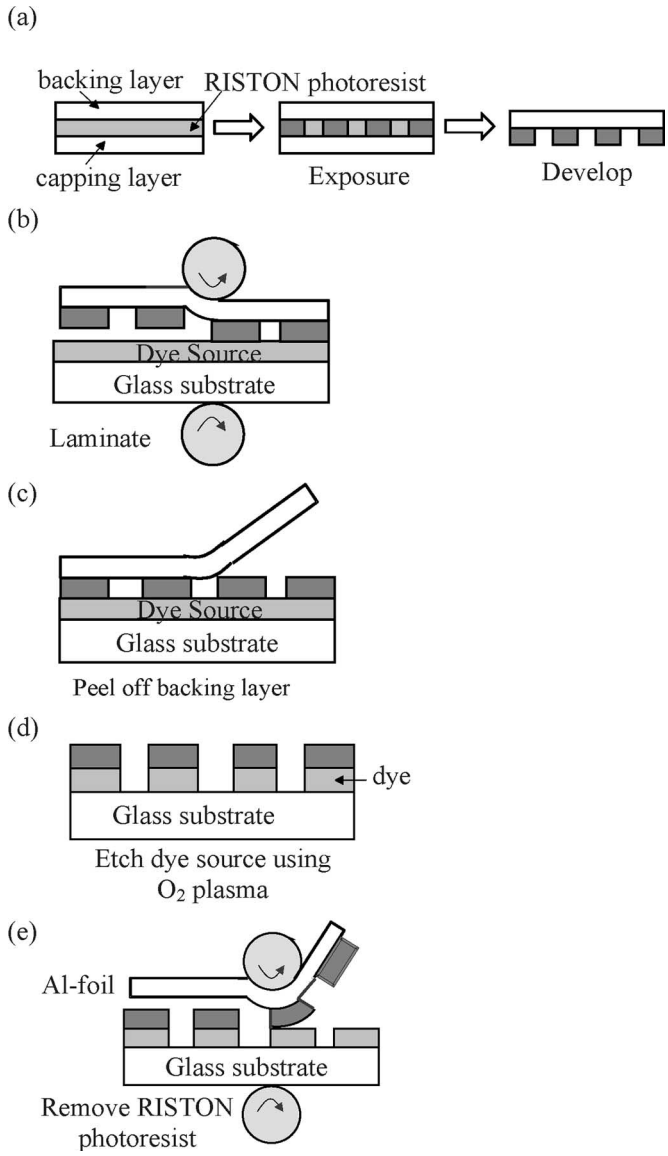

Fig. 2. Fabrication of the printing plate. (a) Pattern RISTON dry photoresist with backing layer remaining as support. (b) Laminate patterned RISTON dry photoresist onto the surface of the dye-doped polymer layer (together with backing layer). (c) Peel off the backing layer to expose the pattern on the dry photoresist. (d) Etch dye-doped polymer using oxygen plasma. (e) Remove the dry photoresist by laminating and peeling off an aluminum foil.

To pattern the dye source, a conventional spun-on photoresist could not be directly applied to the doped Vylon dye source because of undesired interactions between the photoresist processing and the dye source. Therefore, a dry transferable photoresist film RISTON (obtained from DuPont) is used to pattern the dye source layer. A schematic process flow of the dye source patterning is shown in Fig. 2. RISTON is designed to be used as a thick-film photoresist on printed circuit boards (PCB). Normally, it is used by first removing a capping layer and then laminating it onto a PCB, followed by photolithorgraphy while it is attached to the PCB. In our case, the lithography was done first, and the patterned RISTON was transferred. The RISTON was exposed by UV light, the capping layer was peeled off, and the resist was developed [Fig. 2(a)]. The patterned RISTON was laminated onto the dye source at ~ 120 °C, and the backing layer was peeled

off to leave a layer of patterned dry photoresist on the dye source plate [Fig. 2(b) and (c)]. Then, the dye source layer was dry-etched by oxygen plasma using the patterned RISTON film as the mask [Fig. 2(d)]. Finally, an aluminum foil was laminated on top of the RISTON and then peeled off. Since the RISTON film sticks to aluminum much better than to Vylon, the dry photoresist was peeled off together with the aluminum foil, leaving behind the patterned dye source on the glass substrate [Fig. 2(e)]. A different approach, we used the RISTON film on top of the dye as a local diffusion barrier, with the dye source itself not being etched. However, it was found that the photoluminescence (PL) in the host polymer was quenched where it was in contact with the RISTON at elevated temperature during the dye transfer step. This may be due to a contamination in the RISTON entering the host polymer where the films were in contact. As a result, this route was no longer pursued.

C. Dye Printing and Diffusion

To print the dye onto the OLED polymer, the dye source plate and the polymer device plate were aligned and brought into contact in a contact mask aligner, with a thin magnetic steel plate under the device plate. The dye plate was released from the mask holder and secured to the device plate by putting magnets on top of it. The stack of the magnets, the dye plate, the device plate, and the steel plate was then transferred to an oven (70 °C ± 10 °C in vacuum) for the dye printing. At elevated temperature, dye diffuses from the dye source onto the surface of the device polymer. Since the surface roughness of the dye source and the device polymer is ±3 nm, the two layers are in intimate contact at some points with the dye diffusing directly from from one film to another. At other areas, there is a gap between the plates, and the dye evaporates from the source plate, travels a short distance (maximum of 6 nm) in the gas phase, and redeposited onto the surface of the device polymer.

The printing step discussed above left the dye on the surface of the device polymer, presumably due to the device polymer's high glass transition temperature T_g ($\sim$ 120 °C for PVK and PBD mixtures) and the low diffusion coefficient of dye in the polymer matrix [8], [9]. Then, the device plate was put into an acetone vapor ambient for annealing to soften the device polymer to increase the diffusion coefficient [8]. This is because an acetone vapor is absorbed by the polymer and causes it to expand. The glass transition temperature T_g of the polymer is thus greatly reduced, resulting to an increase in the dye diffusion coefficient by many orders of magnitude. The increase is so large that during the acetone vapor "annealing," the dye can diffuse throughout the bulk of the polymer film very quickly even at room temperature. This process is discussed in detail in [8] and [9].

Fig. 3 shows the electroluminescence (EL) spectra of the PVK/PBD/C47 (70.1%/28.7%/0.3% by weight) devices with C6 transferred from a dye source of Vylon layer doped with C6 (4% by weight). The insert plot shows the device structure. C47 is a blue dye with peak emission at 440 nm, and C6 is a green dye with peak emission at 500 nm. For the device made with only the initial printing step (in vacuum at 70 °C for 1 h), only blue emission from C47 present from the initial spin-coating film was obtained. This is because the printed C6 is accumulated at the surface of the polymer film and is not active in the emission process. Conventional annealing to diffuse C6 into the bulk of the device polymer is not desirable because it is too slow: After 4 h at 92 °C, the penetration of C6 into the polymer bulk is still clearly limited, with the C6 concentration at a depth of 100 nm only 9% of that at the surface [8]. Therefore, we chose to employ the solvent-enhanced diffusion process described above. After 60 s of acetone-vapor annealing in a nitrogen–acetone mixture (total pressure = 1 atm and acetone partial pressure = 90 torr), the EL emission has shifted predominantly to green, indicating that C6 is moving into the polymer film. However, a small C47 peak is still observed in the EL spectrum, which maybe due to insufficient C6 in the recombination zone of the device. After a 150-s anneal, the emission is now entirely from C6, the devices are transferred from blue-emitting devices to green-emitting devices by this solvent-enhanced dye diffusion process. In [8] and [9], which focus on the study of this solvent-enhanced dye diffusion process, further details of this process and secondary-ion mass spectroscopy (SIMS) depth profile of the dye in the device polymer are shown. Note that when two dyes are present, PL from both dyes is observed but EL from only the lower energy dye is obtained [10]. This is fortuitous because it allows us to put a blue dye in the emissive device film by the initial spin coating and then achieve patterned RGB EL with only two printing steps for green and red dyes. Dye printing and solvent vapor annealing do not measurably change the device film thickness. Although the film can swell in thickness by 20–30% during the solvent vapor treatment, it shrinks back within minutes after the vapor is removed.

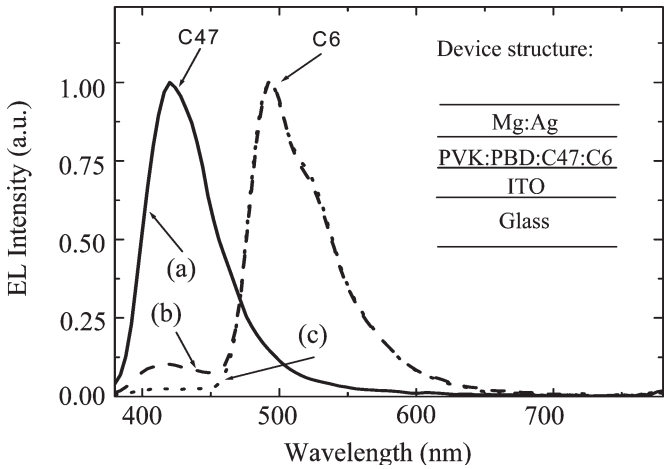

Fig. 3. EL spectra of PVK/PBD/C47 OLEDs with C6 transferred from a dye source of Vylon layer doped with C6 (4% by weight) (a) with only the initial printing step (at 70 °C for 1 h), (b) after 60 s of acetone-vapor annealing, and (c) after 150 s of acetone-vapor annealing at acetone vapor pressure of 92 torr at room temperature. The inset shows the device structure.

D. Stability of the Transferred Dye Pattern

The thermal enhanced diffusion of dye is of great concern in the context of long-term stability of the devices at elevated operating temperature due to power dissipation or storage. We

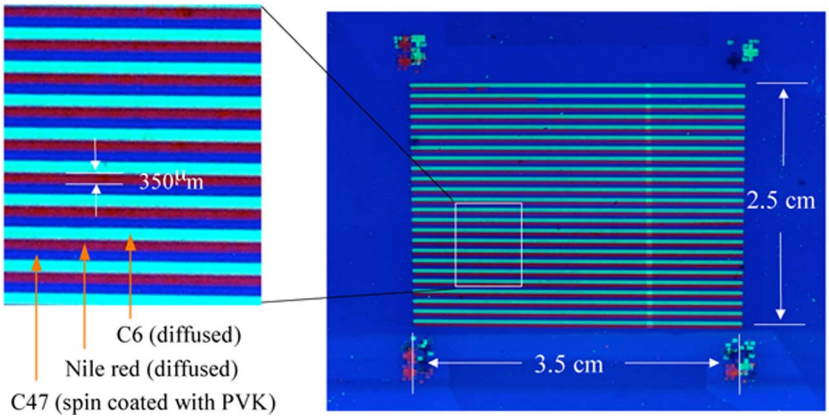

Fig. 4. PL image of a PVK/PBD/dye polymer film with 350-μm-wide blue, green, and red stripes. The blue dye C47 was spin-coated together with the polymer, and the green and red dyes C6 and NR were introduced by two printing steps and a single solvent-enhanced dye diffusion step.

therefore investigated the thermal stability of the dye pattern of C6 lines transferred into a PVK/PBD/C47 film from a C6-doped Vylon layer patterned into lines of 20-μm width with a pitch of 40 μm. The films were annealed at different temperatures, and the change in PL intensity versus distance along the surface was used as evidence of lateral dye diffusion in the polymer. Initially, we observed anomalously high diffusion rates, which were found to be due to the evaporation of dye, and then followed by gas phase transport and redeposition onto undoped areas some distance away. To eliminate this effect, a 60-nm-thick layer of SiN_x was deposited on the polymer surface at 50 °C by plasma-enhanced chemical vapor deposition (PECVD). This solved the anomalous diffusion problem and also helped to reduce any polymer degradation due to contact with air and water vapor at the annealing temperature. The PL image was taken using a fluorescence microscope. The samples were then annealed for 4 h at 90 °C, 105 °C, 120 °C, or 135 °C in nitrogen. After annealing, a PL image was taken again at the same spot and compared to the one taken before the annealing. From the spatial PL intensity profiles taken before and after 4 h of annealing, we were unable to detect any lateral diffusion of the dye at annealing temperatures of 90 °C and 105 °C, but samples annealed at 120 °C and 135 °C showed a slight lateral diffusion. By numerical modeling of the evolution of these profiles, diffusion coefficient for the dyes C6 and NR at 120 °C and 135 °C were extracted and found to be $D = 7 \times 10^{-13} \pm 2 \times 10^{-13}$ cm^2/s for 120 °C and $D = 8 \times 10^{-12} \pm 4 \times 10^{-12}$ cm^2/s for 135 °C. The lower limit for the dye diffusion coefficient within the experimental resolution is 10^{-13} cm^2/s; therefore, no change could be detected at temperatures of 90 °C and 105 °C.

The operating or storage temperature should never exceed the glass transition temperature T_g of the emissive polymer for stability reasons. If we assume, for argument's sake, that the device is held at T_g(120 °C), using the relationship $L = \sqrt{Dt}$, the time needed for a dye to diffuse 1 μm is 115 days. At normal operating or storage temperature, which should be well below the T_g of the device materials, this time span will be significantly longer.

We also examined the stability of the dye pattern during the solvent vapor annealing, which is only of importance during the fabrication process. A 300-μm-wide stripe of C6 was transferred onto a PVK/PBD/C47 film and the full-width at half-maximum (FWHM) of the PL intensity of the stripe before and after the annealing in acetone vapor for 180 s at room temperature was measured. The FWHM of the stripe increases slightly after the acetone annealing by 8 ± 3 μm.

E. Large-Area Patterned Three-Color Polymer Film

Fig. 4 shows a PL image of a PVK/PBD/dye polymer film with blue, green, and red patterns. The blue dye C47 was spin-coated together with the polymer, and the green and red dyes C6 and NR were introduced by two printing steps followed by a single solvent-enhanced dye diffusion step. Each printing step was done in an oven at 70 °C for 1 h in vacuum. The solvent-enhanced dye diffusion is done at room temperature for 150 s in an acetone–nitrogen mixture with a total pressure of 1 atm and an acetone partial pressure of 90 torr. 350 μm-wide RGB color stripes over a 3.5 × 2.5 cm area with excellent color uniformity were achieved. There are indium tin oxide (ITO) stripes underneath the polymer layer along with the color stripes. A full-color passive-matrix display can be made by evaporating cathode stripes perpendicular to the ITO stripes on top of the polymer layer. However, as shown in the next section, the reverse-biased leakage current of these dye-diffused polymer LEDs made with a single layer of 90-nm PVK/PBD/dye is too high to make devices suitable for passive-matrix application.

III. Device Characteristics and Optimization

A. Single-Layer Device I–V Characteristic After Acetone Vapor Annealing

OLEDs were fabricated by evaporated Mg:Ag (10:1)/Ag cathodes through a shadow mask to create large-area test devices (2 mm^2 circles on unpatterned ITO) onto the doped polymer film. Fig. 5 shows the I–V characteristics of the PVK/PBD/C47 devices with C6 transferred from a uniform dye source of Vylon layer doped with C6 (4% by weight in the final film). The photocurrent produced by a photodiode collecting the light emitted from the OLED was also shown.

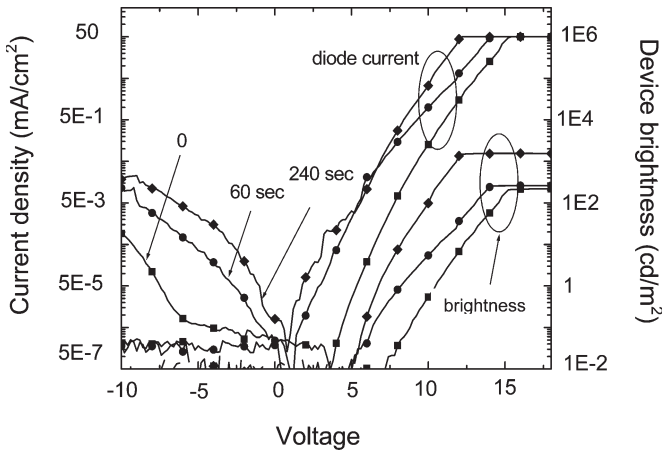

Fig. 5. I–V characteristics of the PVK/PBD/C6 devices annealed in acetone vapor (partial pressure is 92 torr) for different times of devices with C6 transferred from a uniform dye source of Vylon layer doped with C6 (4% by weight in the final film).

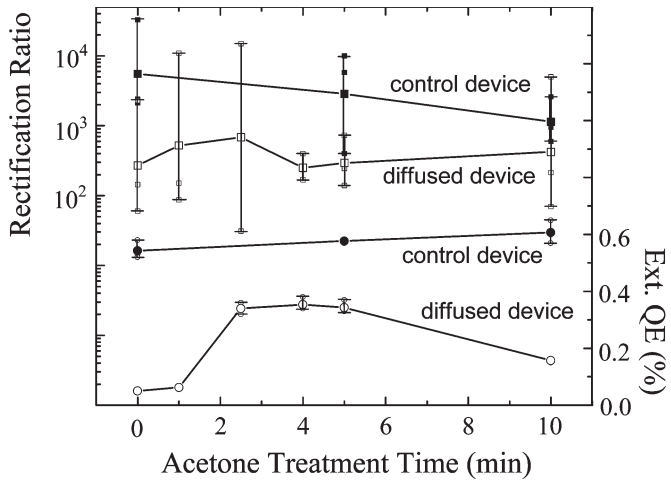

Fig. 6. External quantum efficiency (circles) and the rectification ratio (squares) as a function of exposure time to acetone vapor (partial pressure is 92 torr at room temperature). Control devices (solid symbols) are devices with C6 in the spun-on solution, and diffusion devices (open symbols) are devices with transferred C6.

Based on previous calibration, the external quantum efficiency of the OLEDs can be estimated from this photocurrent. A device with only the initial thermal printing step (in vacuum at 70 °C for 1 h) shows a very low photocurrent and thus a low external quantum efficiency (0.04%) because the printed dye is accumulated at the surface of the polymer film and is not active in the emission process. After annealing in acetone vapor for 60 s in a nitrogen–solvent mixture, the external quantum efficiency increases a bit to 0.06%. After 240 s of annealing, the external quantum efficiency improved by nearly an order of magnitude to 0.35%. Secondary ion mass spectroscopy (SIMS) study shows that now the dye is homogeneously distributed throughout the polymer film [8], [9]. The homogeneous distribution of the dye throughout the polymer film is similar to the case of the spin-on polymer with dye contained in the solution, which produced the best device efficiency because now all the dye is active in the emission process. The external quantum efficiency of these devices is comparable to those of the devices with dye contained in the spin-on solution (not printed), as shown in Fig. 6.

However, Fig. 5 also shows that the reverse-biased current of the devices treated with acetone vapor increases with the exposure time to the acetone vapor drastically. This is also true for control devices with dye contained in the spin-on solution and not printed. The rectification ratio γ, which is defined as the ratio of the forward-biased current at 10 V over the reversed-biased current at -10 V, shows this trend in Fig. 6. The reason for the increase of the reverse-biased current has not been investigated. In any case, an increased leakage current is especially harmful for passive-matrix display applications because of the resulting inability to individually address single devices [15].

B. Bilayer Devices

To reduce the reverse-biased leakage current of the single-layer doped polymer LEDs, an electron transport layer (ETL) was added on top of the polymer layer after the introducing of the dyes into the polymer matrix. Tris-8-hydroxyquinoline aluminum (Alq_3) was chosen for this ETL because it has good electron conductivity and a low highest occupied molecular orbital (HOMO), thus resulting to an increased barrier for hole injection [16]. When a single-layer PVK-based OLED is under reverse bias, the hole injection barrier (1.8 eV) is lower than the electron injection barrier (2.5 eV) [2], [16], and the dominant leakage current comes from the hole current. Alq_3 has a HOMO level that is 0.3 eV lower than that of PVK, and an additional Alq_3 layer increases the thickness of the device structure, thus decreasing the electrical field under the same bias, so adding an Alq_3 layer can suppress hole injection under reverse-bias, thus reducing the reverse leakage current. In addition, the Alq_3 layer also increases the efficiency of the OLEDs because it moves the cathode away from the emissive dyes to reduce cathode quenching of the excitons via a dipole–metal interaction [17] and balances electron and hole transport to raise efficiency.

Bilayer devices were first made by locally doping the PVK-based film as demonstrated earlier. A blanket Alq_3 film was then evaporated on top of the PVK-based layer and was followed by cathode deposition. Fig. 7 shows the typical I–V characteristics of the single-layer and bilayer devices doped with C6. The leakage at 20 V reverse bias is decreased by almost four orders of magnitude, and the forward current at a given bias increases by a factor of 2, greatly increasing the rectification ratio at $\pm$ 10 V to $\sim 1 \times 10^6$.

C. Hole/Exciton Blocking Layer

While the electrical properties of the bilayer devices are attractive, the optical emission properties are not. Single-layer devices doped with C47 emit blue light (peak emission at 440 nm) [Fig. 8(a)]. Bilayer devices doped with C47 in the polymer emit predominantly at 530 nm (green) with only a small peak at 440 nm [Fig. 8(b)]. This undesired green peak is thought to be due to emission from the Alq_3. A device made with undoped PVK as an Hole Transport Layer (HTL) and evaporated Alq_3 as an ETL and emitting layer emits in this same range [Fig. 8(c)].

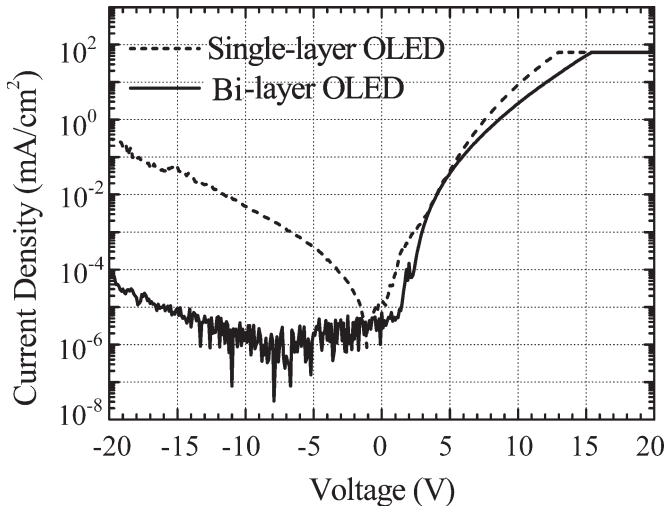

Fig. 7. Typical I–V characteristics of the single-layer (dashed line) and bilayer (solid line) devices doped with green dye C6, where the PVK/PBD/C6 layer is made by spin coating.

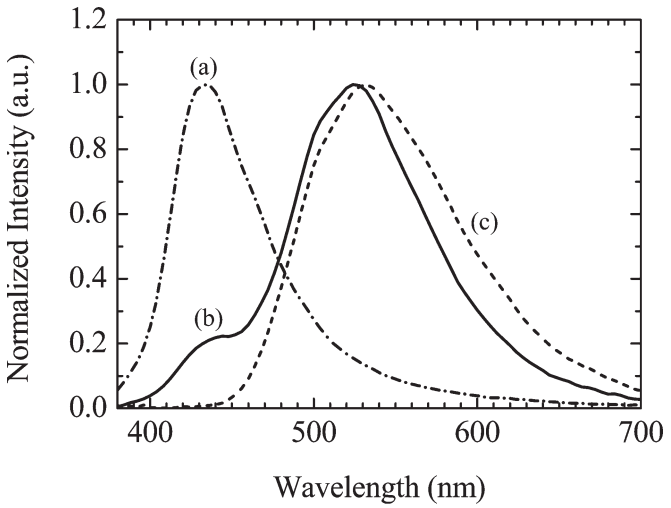

Fig. 8. Normalized EL spectra of (a) single-layer device of 90 nm PVK/PBD/C47 (dash-dotted line), (b) bilayer device of 90 nm PVK/PBD/C47 + 40 nm Alq_3 (solid line), and (c) Alq_3 emission reference (dashed line).

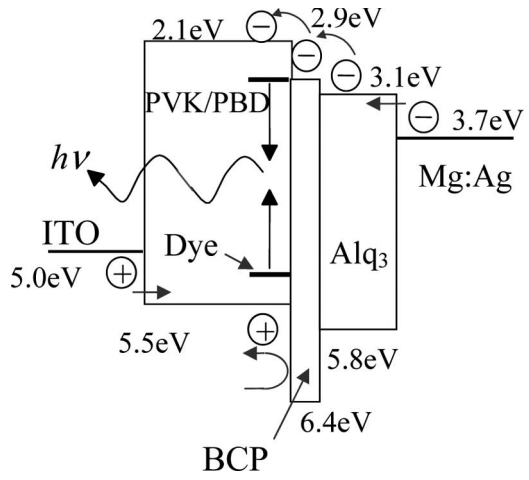

Fig. 9. Schematic band diagram of the trilayer OLED structure with PVK:PBD:Dye/BCP/Alq_3.

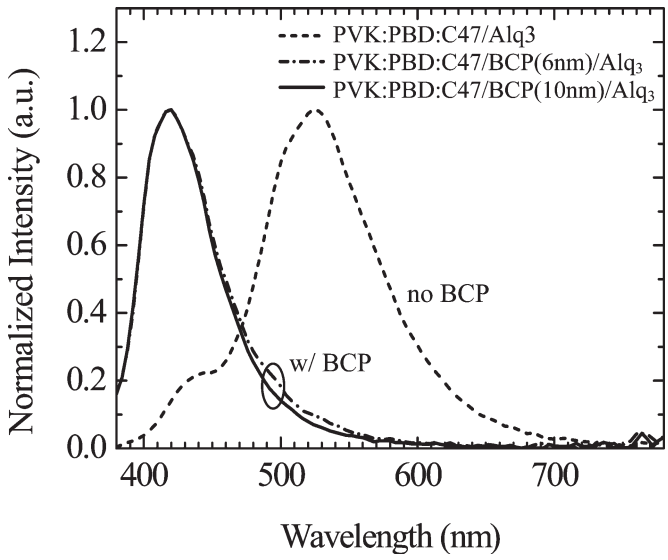

Fig. 10. EL spectra of the blue dye-doped OLEDs with or without BCP hole/exciton blocking layer.

The following two processes can cause this undesired green Alq_3 emission in devices in which the PVK is doped with only C47: 1) Due to the lower energy gap in the Alq_3, excitons formed in the polymer layer will migrate into the Alq_3 layer and recombined there or 2) holes can be injected from the PVK layer into the Alq_3 layer and form excitons directly in Alq_3. Therefore, the dye in the polymer does not control the emission color.

To eliminate the OLED color problem from Alq_3 emission, and to confine the light emission within the dye-doped polymer layer, holes and excitons must be prevented from entering the Alq_3 layer. For this purpose, we placed a thin hole/exciton blocking layer (HBL/EBL) between the doped-polymer layer and the Alq_3 layer. 2,9-Dimethyl-4,7-diphenyl-1, 10-phenanthroline (BCP) was used for this blocking layer because it satisfies the bandgap requirement for this hole/exciton blocking layer [16], [18]. As shown in Fig. 9, BCP has a low HOMO to block the holes from entering the Alq_3 layer. The barrier from PVK to BCP is 0.9 eV versus only 0.3 eV from PVK directly into Alq_3. Furthermore, the high bandgap of BCP confines the excitons within the polymer layer (3.6 eV in BCP versus 2.7 eV in Alq_3). BCP also has a low-enough electron barrier to allow electrons to pass through and enter the polymer layer because the LUMO of BCP (2.9 eV) is between the LUMO of the Alq_3(3.1 eV) and the LUMO of the PBD (2.1 eV) doped in the PVK for electron transport [2], [16].

Fig. 10 shows the spectra of the blue dye-doped devices with a BCP hole/exciton blocking layer with different thicknesses. The dominant emission is green without the BCP layer, and with a thin layer of BCP of 6 nm or 10 nm, the emission is all from the blue dye; no green Alq_3 emission is observed as desired. Furthermore, the addition of this thin blocking layer does not increase the operation voltage of the OLEDs. Individual RGB polymer LEDs have been fabricated with this trilayer structure (not yet integrated). The devices begin with a 90-nm-thick polymer blend layer of PVK/PBD and a fluorescence dye (Nile red for red devices, Coumarin 6 for green devices, and

TABLE I
COMPARISON OF THE EL EFFICIENCIES AND THE CURRENT RECTIFICATION RATIO AT ±10 V OF THE SINGLE-LAYER AND TRILAYER DEVICES WITH RED, GREEN, AND BLUE DYE DOPANTS, RESPECTIVELY

		Blue (C47)	Green (C6)	Red (Nile red)
η_{ext} (%)	Single-layer	0.13%	0.70%	0.61%
	Tri-layer	0.34%	1.1%	0.95%
Rectification ratio @ ±10V	Single-layer	1.5e4	1.3e3	7.4e3
	Tri-layer	2.4e6	1.3e6	8.7e5

Coumarin 47 for blue devices), which is deposited on top of the ITO layer by spin coating. The typical dye concentration was 0.3% by weight. Then, a thin (6 nm) BCP layer as a hole/exciton blocking layer and a 40-nm-thick Alq_3 layer as an ETL are deposited sequentially by thermal evaporation. A 150-nm thick Mg:Ag (10:1)/Ag layer is deposited as the OLED cathode. The EL spectra of the fabricated blue, green, and red trilayer devices show peak wavelengths at 440, 500, and 590 nm, respectively. Compared with the devices without the BCP layer in Fig. 8, the peaks of the RGB devices are well defined and do not show the contamination of color from the Alq_3 emission. These trilayer devices have very high rectification ratio ($> 10^6$ for green devices) and a higher external quantum efficiency compared to the single-layer devices (1.1% versus 0.7% for green devices) (Table I).

D. Optimization of Device Efficiency

It was initially observed that devices made from printing plates with 2% dye in Vylon (as spin-coated) that had been through this patterning process had lower quantum efficiencies than devices made from a printing plate with the same amount of 2% dye in Vylon that was not patterned (0.22% versus 0.51%; Fig. 13). This was found to be due to the loss of a large amount of dye (presumably by diffusion) from the Vylon to the RISTON during the lamination of the patterned RISTON to the dye source plate [Fig. 2(b)]. For adhesion, the lamination was done at ~ 120 °C for ~ 5 min. This step depleted the dye source, so less dye was available for subsequent transfer to devices. The SIMS of the green dye C6-doped Vylon films show that about 70% of dye in the dye source plate was lost due to the patterning process (Fig. 11).

The OLED electrouminescence efficiency is strongly dependent on the dye concentration in the polymer film [19]. The EL efficiency increases with dye concentration initially because more excitons can be formed on the dye due to an increased number of dye molecules. However, at a certain dye concentration, the OLED EL efficiency reaches its peak. An excess dye concentration leads to dye quenching and thus a lower EL efficiency. Further, the EL is much more sensitive to the dye concentration than the PL [14]. In the trilayer devices, 0.3% dye in PVK by weight yielded the highest EL external quantum efficiency of the devices, which was 1.1% for green devices. To achieve this optimum final device concentration, we determined experimentally the optimum dye source concentration in the printing stamp to be 2% dye in Vylon by weight for dye transfer at 70 °C for 60 min when using an unpatterned spin-coated dye source.

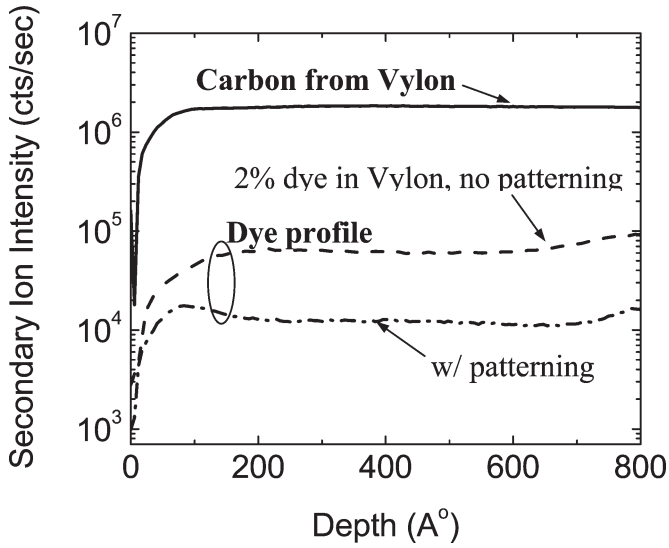

Fig. 11. SIMS profiles of the green dye C6-doped Vylon films before and after patterning process.

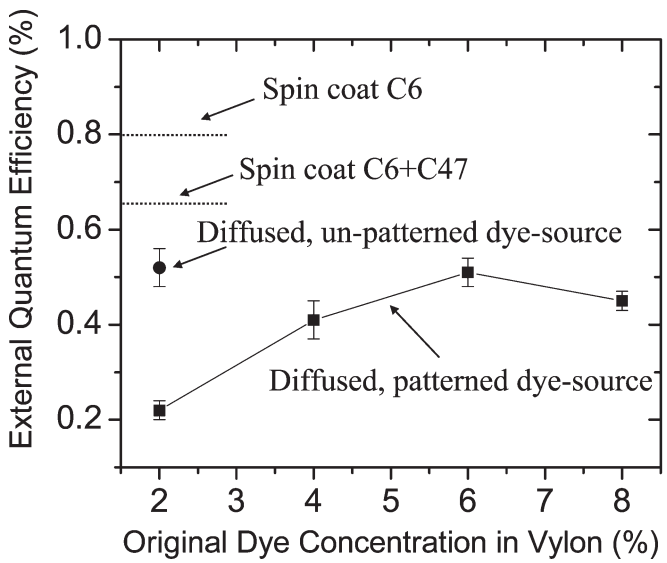

Fig. 12. EL quantum efficiencies of green devices fabricated with different dye doping methods.

Since there is dye loss due to the patterning process, the initial dye concentration in Vylon needed to be increased when making a patterned printing plate. We then made diffused C6 devices with patterned dye sources from 2%, 4%, 6%, and 8% initial dye in Vylon and measured the EL external quantum efficiency of these devices (with trilayer structures as in Fig. 9). The devices made using dye source with 6% initial C6 in Vylon yielded the highest EL external quantum efficiency (0.51%), which is the same as that of the devices made using unpatterned dye source of the optimum 2% C6 in Vylon (Fig. 12).

E. Full-Color Passive-Matrix Test Array

Using the steps of this dye-printing solvent-enhanced diffusion, and the trilayer device structure, a full-color passive-matrix test array was fabricated with integrated RGB emitting

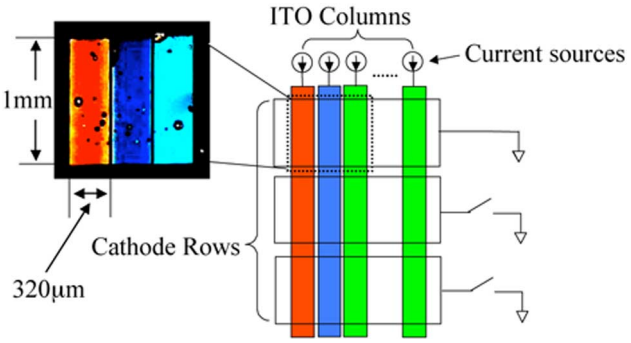

Fig. 13. EL micrograph of an RGB pixel from a small passive-matrix test array fabricated using dry dye printing and trilayer structure.

devices. First, ITO was patterned into 320-μm-wide stripes as column electrodes by wet etching. A blue-doped (C47) PVK layer was spin-coated, followed by C6 (green) and Nile red (red) dry printing and a solvent-assisted diffusion step. The RGB color stripes were aligned with the ITO stripes. Then, a thin 6-nm BCP layer and a 40-nm-thick Alq_3 layer were deposited by thermal evaporation on top of the dye-doped PVK layer. Finally, a 150-nm-thick Mg:Ag (10:1)/Ag layer was deposited as the OLED cathode, with a shadow mask to pattern the cathode into stripes perpendicular to the ITO stripes as row electrodes. A 3-row by 15-column 3-color passive-matrix test array was fabricated with 100% pixel yield. Fig. 13 shows a schematic diagram of the test array and an optical micrograph of one pixel. Although the cathode contains dark spot defects, the color of each subpixel is well defined, and the brightness of the individual pixels could be well controlled.

IV. Discussion

Our final device structure is unusual for a patterned device. It is not uncommon to find a small-molecule ETL on top of polymer HTL [20], [21]. However, in our case, it is the hole transport layer that is patterned as the color emitter, and the ETL is uniform. This is the opposite of the usual approach in three-color structures based on small molecules [1]. This results from the fact that for several reasons, printing steps are most amenable to polymers than small molecules, and that the polymer layer was deposited before the small molecules because of concerns that the polymer processing and printing would damage underlying small molecules. (We tried at length to adopt the printing process shown in this paper to dope Alq_3, but the solvent vapor step caused recrystallization of the Alq_3.) While polymers are amenable to printing, small molecules are more easily used to control transport properties and the thickness of the layers. Thus, our general approach represents a novel combination to exploit the best properties of both small-molecule films (for transport and band diagram) and polymer films (for printability) for OLEDs.

V. Summary

Dry dye printing from a prepatterned printing stamp followed by solvent-enhanced dye diffusion was used to locally dope a previously spin-coated polymer film with different dyes to fabricate side-by-side RGB OLED subpixels for a full-color display. To reduce reverse leakage current and improve efficiency, a novel trilayer OLED structure, which consists of an additional Alq_3 ETL layer and a BCP hole/exciton blocking layer was developed. The BCP layer confines the light emission to the doped polymer layer. The EL external quantum efficiency of the devices was optimized by the dye concentration in the printing plate. Devices with this trilayer structure and the optimized dye source demonstrate higher external quantum efficiency ($\sim 1\%$) and an extremely low reverse leakage current (rectification ratio of 10^6 at $\pm$ 10 V). This device architecture demonstrates a new approach for combining the printability of polymer with the optimum transport capability of small organic molecules to achieve high-performance OLEDs.

References

[1] C. W. Tang, S. A. Vanslyke, and C. H. Chen, "Electroluminescence of doped organic thin films," *J. Appl. Phys.*, vol. 65, no. 9, pp. 3610–3616, May 1989.

[2] C. C. Wu, J. C. Sturm, R. A. Register, J. Tian, E. P. Dana, and M. E. Thompson, "Efficient organic electroluminescent devices using single-layer doped polymer thin films with bipolar carrier transport abilities," *IEEE Trans. Electron Devices*, vol. 44, no. 8, pp. 1269–1281, Aug. 1997.

[3] T. R. Hebner and J. C. Sturm, "Local tuning of organic light-emitting diode color by dye droplet application," *Appl. Phys. Lett.*, vol. 73, no. 13, pp. 1775–1777, Sep. 1998.

[4] J. Kido, S. Shirai, Y. Yamagata, and G. Harada, "Multicolor polymer electroluminescent devices," presented at the Mater. Res. Soc. Symp., San Francisco, CA, 1999.

[5] K. Tada and M. Onoda, "Three-color polymer light-emitting devices patterned by maskless dye diffusion onto prepatterned electrode," *Jpn. J. Appl. Phys.*, vol. 38, no. 10A, pp. L1143–L1145, Oct. 1999.

[6] F. Pschenitzka and J. C. Sturm, "Three-color organic light-emitting diodes patterned by masked dye diffusion," *Appl. Phys. Lett.*, vol. 74, no. 13, pp. 1913–1915, Mar. 1999.

[7] ——, "Patterned dye diffusion using transferred photoresist for polymer OLED displays," *Proc. SPIE*, vol. 59, pp. 4105–4115, 2000.

[8] ——, "Solvent-enhanced dye diffusion in polymer thin films for color tuning of organic light-emitting diodes," *Appl. Phys. Lett.*, vol. 78, no. 17, pp. 2584–2586, Apr. 2001.

[9] T. Gravis-Abe, F. Pschenitzka, H. Z. Jin, R. A. Register, and J. C. Sturm, "Solvent-enhanced dye diffusion in polymer thin films for polymer light-emitting diode application," *J. Appl. Phys.*, vol. 96, no. 12, pp. 7154–7163, Dec. 2004.

[10] T. R. Hebner, C. C. Wu, D. Marcy, M. H. Lu, and J. C. Sturm, "Ink-jet printing of doped polymers for organic light emitting devices," *Appl. Phys. Lett.*, vol. 72, no. 5, pp. 519–521, Feb. 1998.

[11] M. L. Williams, R. F. Landel, and J. D. Ferry, "The temperature dependence of relaxation mechanisms in amorphous polymer and other glass-forming liquids," *Amer. Chem. Soc.*, vol. 77, pp. 3701–3707, 1995.

[12] T. E. Shearmur, D. W. Drew, A. S. Clough, M. G. D. van der Grinten, and A. T. Slark, "Study of dye diffusion using Rutherford backscattering," *Polymer*, vol. 37, no. 13, pp. 2695–2700, 1996.

[13] T. Shimoda, K. Morii, S. Seki, and H. Kiguchi, "Inkjet printing of light-emitting polymer displays," *Mater. Res. Soc. Bull.*, vol. 28, no. 11, pp. 821–827, Nov. 2003.

[14] F. Pschenitzka and J. C. Sturm, "Excitation mechanisms in dye-doped organic light-emitting devices," *Appl. Phys. Lett.*, vol. 79, no. 26, pp. 4354–4356, Dec. 2001.

[15] D. Braun, "Crosstalk in passive matrix polymer LED displays," *Synth. Met.*, vol. 92, no. 2, pp. 107–113, Jan. 1998.

[16] I. G. Hill and A. Kahn, "Organic semiconductor heterointerfaces containing bathocuprione," *J. Appl. Phys.*, vol. 86, no. 8, pp. 4515–4519, Oct. 1999.

[17] V. Bulovic, V. B. Khalfin, G. Gu, P. E. Burrows, D. Z. Garbuzov, and S. R. Forrest, "Weak microcavity effects in organic light-emitting devices," *Phys. Rev. B, Condens. Matter*, vol. 58, no. 7, pp. 3730–3740, Aug. 1998.

[18] R. S. Deshpande, V. Bulović, and S. R. Forrest, "White-light-emitting organic electroluminescent devices based on interlayer sequential energy transfer," *Appl. Phys. Lett.*, vol. 75, no. 7, pp. 888–890, Aug. 1999.
[19] C. C. Wu, J. C. Sturm, R. A. Register, and M. E. Thompson, "Integrated three-color organic light-emitting devices," *Appl. Phys. Lett.*, vol. 69, no. 21, pp. 3117–3119, Nov. 1996.
[20] C. C. Wu, J. K. M. Chun, P. E. Burrows, J. C. Sturm, M. E. Thompson, S. R. Forrest, and R. A. Register, "Poly(P-phenylene vinylene)/tris (8-hydroxy)quinoline aluminum heterostructure light emitting diode," *Appl. Phys. Lett.*, vol. 66, no. 6, pp. 653–655, Feb. 1995.
[21] Z. Xie, C. Qiu, H. Chen, B. Tang, M. Wong, and H. Kwok, "High efficiency polymer-based electrophosphorescent organic light-emitting diode," in *Proc. SID Tech. Dig.*, 2003, vol. 34, pp. 512–515.

K. Long (M'03), photograph and biography not available at the time of publication.

F. Pschenitzka, photograph and biography not available at the time of publication.

M.-H. Lu (S'97–M'01), photograph and biography not available at the time of publication.

James C. Sturm (M'80–S'81–SM'95–F'01), photograph and biography not available at the time of publication.